Indian Journal of Engineering & Materials Sciences
Vol. 17, February 2010, pp. 20-26

Comparative study on the suitability of feature extraction techniques for tungsten inclusion and hotspot detection from weld thermographs for on-line weld monitoring

N M Nandhitha[a]*, N Manoharan[a], B Sheela Rani[a] , B Venkatraman[b], P Kalyanasundaram[b] & Baldev Raj[b]
[a]Sathyabama University, Rajiv Gandhi Road, Jeppiaar Nagar, Chennai 600 119, India
[b]Indira Gandhi Centre for Atomic Research, Kalpakkam 603 102, India

Received 8 September 2008; accepted 15 February 2010

Welding is the most commonly used technique for joining metals in industries. In spite of various technological advances defects do occur in welds. Post non-destructive testing (NDT) techniques assess the quality of weld after completion of welding process. Monitoring and controlling weld parameters during welding can avoid the defect or if the defect is already intolerable the welding process can be stopped there to save time and money. It is thus necessary to develop an automated on-line welding system to make the correct decision. Weld thermographs are acquired on-line with IR camera. Effective feature extraction algorithms are to be developed to isolate and quantify the defect features from thermographs. This paper compares the effectiveness and suitability of three different feature extraction algorithms namely discontinuity based detection (conventional), region growing and Euclidean distance based color image segmentation developed for on-line monitoring and control. Tungsten inclusion and different depths of penetration thermographs are the database considered for defect feature extraction. Online weld monitoring necessitates a standardized feature extraction technique that works well irrespective of the size and shape of defect. Hence, comparison is based on the accuracy of the results, parameter independency and image independency. It is found that feature extraction by Euclidean distance based segmentation is best suited for on-line weld monitoring as it is parameter independent and can be standardized for a defect.

Keywords: Thermographs, Depths of penetration, Tungsten inclusion, Edge detection, Region growing, Euclidean distance, Feature vectors

Gas tungsten arc welding (GTAW) is the most commonly used welding technique in industries to join metals. It is an arc welding process wherein the coalescence is produced by heating the job with an electric arc struck between the tungsten electrode and the job. A shielding gas is used to prevent atmospheric contamination of the molten weld pool. In spite of the numerous advances in the science and technology of welding, failures do occur and weld is still considered to be the weakest portion. The most commonly occurring weld defects that cause serious problem are lack of penetration and tungsten inclusion. This is because the formation of the weld is affected by a number of process parameters which make it difficult to ensure the quality of weld. Hence, it is necessary to develop an automated defect detection system to assess weld quality. However, post NDT techniques assess the quality of weld after completion of welds. It results in wastage of money, manpower and time. This problem can be overcome by developing an on-line weld defect monitoring system that produces defect free welds. In order to develop such a system it is necessary to select a suitable sensor to acquire weld images.

Of the various sensors available in literature for capturing the weld images, infrared thermography (IRT) is best suited for acquiring weld images during and after welding. Infrared thermography may be defined as non-destructive, non-intrusive, non-contact mapping of thermal patterns on the surface of the objects. It is used to diagnose the thermal behaviour and thereby to assess the performance of the equipment and the integrity of the materials, products and processes.

Thermal maps produced by infrared thermal imaging instruments are called thermographs. These thermographs are stored in computers for defect detection. A thermograph appears symmetrical and

*Corresponding author (E-mail: nandhi_n_m@yahoo.co.in)

uniform in the absence of anomalies. On the other hand defects appear as abrupt high or low temperature regions in a thermograph. As these variations best describe the defects, feature extraction techniques can be developed to determine these temperature differences.

Numerous groups worldwide have used infrared investigation techniques in the inspection of subsurface defects and features, thermo-physical properties, coating thickness and hidden structures. Thermographs are used to the control of welding process problems, such as arc misalignments[1]. Infrared sensors are best suited for weld quality detection as the perturbations that arise due to variations in arc positioning, heat input and the presence of contaminants distinctly manifests itself as differences in the spatial and temporal surface temperature distributions. Hence, image analysis techniques can be developed to quantify the changes in the temperature distribution there by enabling adaptive welding techniques for automated weld control[2]. Infrared thermography was used for on-line control of torch path in robotic gas tungsten arc welding. Thermographs were transmitted to a central computer where an image processing algorithm was developed to determine the torch from the joint and also transmitted the corrective action to control the torch path. However, the developed method was suitable for only single V-groove configurations[3]. Infrared sensing and computer image processing techniques can be used as a feasible method to improve the welding process through dynamic control of joint penetration parameters. An infrared camera was mounted on the front side of the weld pool and surface temperature distributions surrounding the weld pool were measured during the welding process. Welding parameters were varied to obtain different depths of penetration and the corresponding temperature distributions were noted. However relative temperature with respect to a specific chosen temperature was considered instead of the absolute temperature[4]. Infrared sensing techniques were used to track curved contours of joints with a gap in fusion reactor welding. It was found that a gap in a weld joint produce a significant drop in the measured Infrared intensity or temperature and this temperature reduction can be used to determine the size and position of a joint gap[5]. Infrared thermography is highly suitable for sensing variations in bead width and depth of penetration due to variations in plate thickness, shielding gas composition and minor element content in GTAW[6]. Different passive and active thermographic techniques are used for defect detection. Active techniques include pulse thermography, lockin thermography, pulsed phase thermography and vibrothermography[7-9]. Thermographs reveal significant features of thermal conditions that cannot be modeled theoretically in practical sense[10]. Quantification of thermographs is achieved by image processing algorithm through histogram equalization, image segmentation and morphological image processing[11]. Phase and amplitude of the image are obtained by fast Fourier transform and it was found that phase profile for a defect exhibits a distinctive inflexion point at blind frequency and hence the defects are quantified[12]. In contrast to the conventional contrast based methods, thermographic signal reconstruction method was used for the analysis of thermographic data to increase detectability and provide automated pass/fail processing in pulsed thermography[13].

From the literature, it is found that infrared thermography is extensively used for weld defect detection. Thermograph is the thermal map of temperature variations and is relatively easy to interpret. However, manual interpretation of thermographs is subjective even for skilled thermologists. Hence, it is necessary to develop automated defect feature extraction techniques which can then be adopted for on-line monitoring and control.

Thermographs Database

Image database was collected from IGCAR, Kalpakkam to understand the nature and characteristics of thermographs. Moreover, these thermographs were used for developing automated feature extraction techniques for automated weld defect detection. Tungsten inclusion thermographs and thermographs depicting different depths of penetration are considered in this work. Tungsten inclusion occurs when a piece of tungsten gets entrapped in the weld pool. It is caused by very high welding current is used for the electrode or unstable arc or when the electrode momentarily touches the weld pool. In all the above thermographs, these defects are of different intensities when compared to the weld region. Different depths of penetration occur when the torch current decreases or torch speed increases. Thermographs depicting tungsten inclusion and depths of penetration are shown in Figs 1 and 2 respectively. In the absence of defects, temperature variation in thermographs is uniform and symmetrical. A defect appears as abrupt variation in temperature.

Tungsten appears as a relatively high temperature region. In different depths of penetration thermographs, it is found that the size and shape of the hot spot varies as the depth of penetration varies.

Development of Feature Extraction Techniques

Thermographs depicting defects are acquired off-line and feature extraction software is developed for defect detection and quantification.

Discontinuity based feature extraction technique

Thermographs are converted from colour domain to gray scale domain in order to reduce the computational complexity[14]. Image enhancement is done with averaging Gaussian and Gaussian filters to highlight the defect region in thermographs. Image segmentation by edge detection is performed on these thermographs with suitable filters (Sobel/Prewitt/Canny). After edge detection, post processing (dilation, region growing and erosion) is done to remove the undesirable regions. Dilation is performed on the edge detected image to bridge the gap between the edge pixels. Region growing is performed on the dilated image to differentiate the region of interest pixels from the background pixels. Erosion is performed on the region filled image to isolate the defect or the region of interest. The flowchart is as shown in Fig. 3.

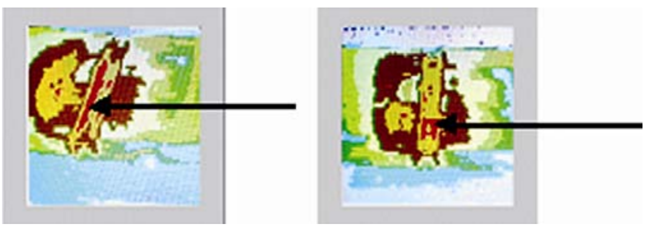

Fig. 1—Tungsten inclusion (rod and gauge shaped)

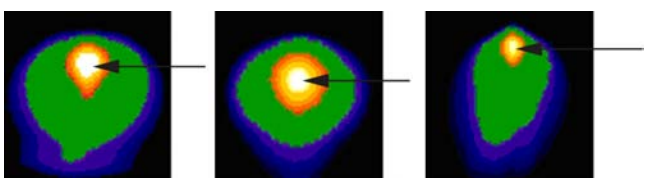

Fig. 2—Depth of penetration thermographs (100%, 80% and 60)

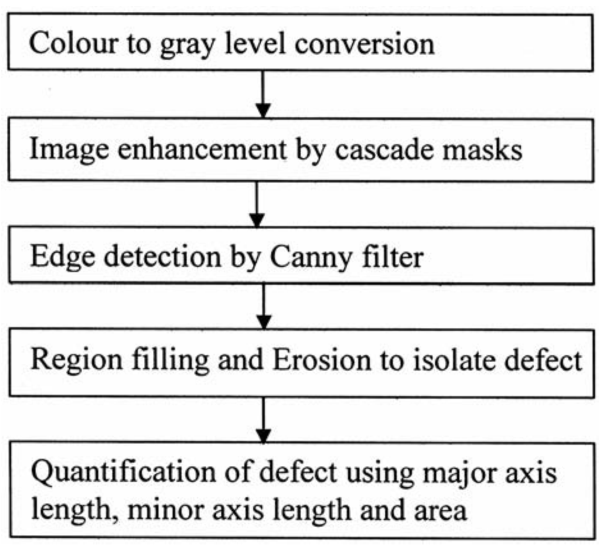

Fig. 3—Feature extraction by discontinuity based detection

Region growing based feature extraction technique

The algorithm involves colour to gray level conversion, selecting a seed pixel, determining the threshold value, finding out the difference between every image pixel and the selected seed pixel and appending the image pixel whose difference is less than or equal to the threshold. The flowchart of the algorithm is as shown in Fig. 4.

Euclidean distance based colour image segmentation

This technique is proposed for pseudo colour thermographs, i.e., it works directly on colour images. It involves selecting an average pixel in the region of

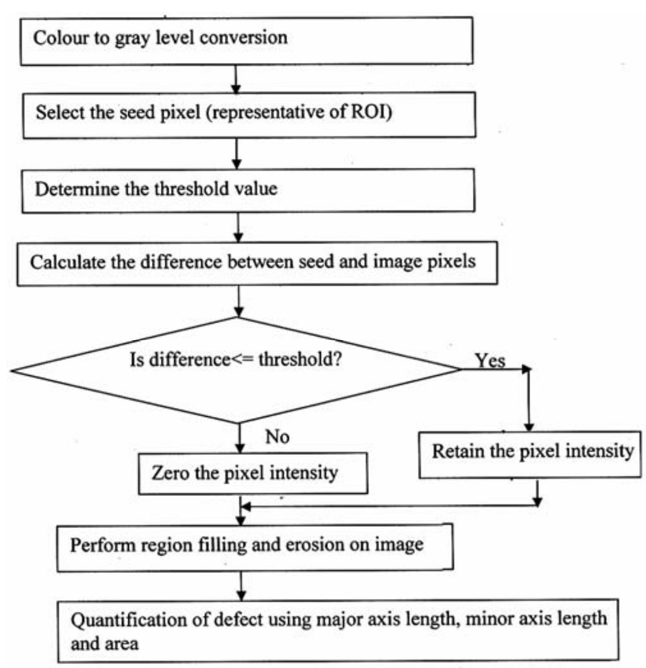

Fig. 4—Feature extraction by region growing

interest (three different values for red, blue and green domains, fixing a threshold value, determining the Euclidean distance[14] for every image pixel and the average pixel, appending the image pixel whose Euclidean distance is less than or equal to the threshold value. The flowchart is shown in Fig. 5.

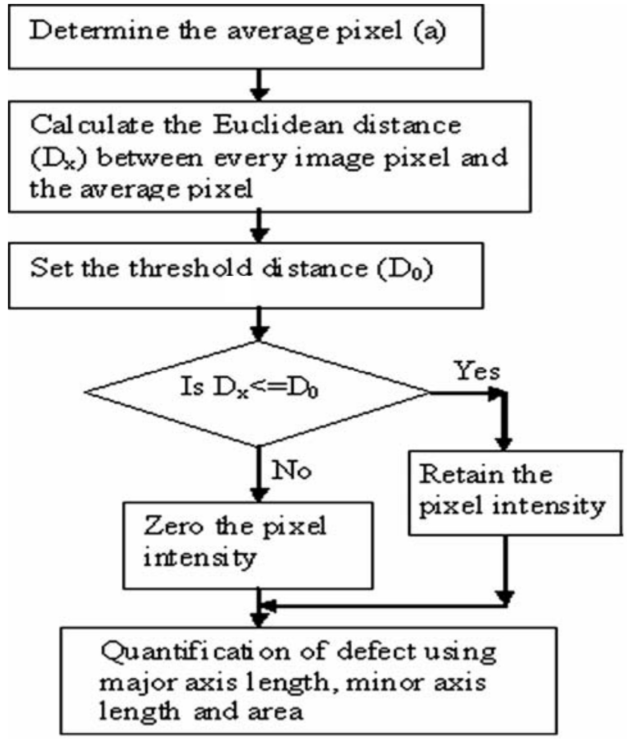

Fig. 5—Feature extraction by color image processing

Results and Discussion

The developed defect feature extraction techniques are applied on tungsten inclusion thermographs and thermographs depicting different depths of penetration. Various parameters involved in defect feature detection are as shown in Table 1.

Graythreshold is the global threshold value calculated using Otsu's method, which chooses the threshold to minimize the intraclass variance of the thresholded black and white pixels.

Defect feature extraction by discontinuity based technique involves five different parameters namely enhancing filters, edge detection masks, structuring elements for dilation, region growing and erosion thereby making this technique parameter dependent. As is evident from rows 3-7, even for images of same

Table 1—Parameters involved in feature extraction techniques

Feature extraction techniques	Parameters/ Defects	Depth of penetration			Tungsten inclusion	
		100%	80%	60%	Rod shaped	Gauge shaped
Discontinuity based detection	Enhancement	-	-	-	Average, Gaussian [5 5], [3 3]	Gaussian, Average [5 5], [5 5]
	Segmentation (filter & Threshold)	Sobel graythreshold *0.35	Sobel graythreshold *0.15	Sobel graythreshold *0.15	Canny graythreshold *0.15	Canny graythreshold *0.35
	Dilation	-	-	No dilation	Horizontal line (2 pixels)	Horizontal line (2 pixels)
	Region Filling	holes	holes	holes	holes	holes
	Erosion	Square (4 pixels)	Square (4 pixels)	Square (2 pixels)	Diamond (1 pixel)	Diamond (2 pixels)
Region growing	Enhancement	-	-	-	-	-
	Segmentation	Seed intensity is 0.9961, Threshold =0.04			Seed intensity is 0.38, Threshold = 0.04	
	Dilation	-	-	-	Horizontal & vertical line (1,2 pixels)	-
	Region filling	-	-	-	holes	holes
	Erosion	-	-	-	Diamond (1 pixel)	Rectangle [3 3]
Euclidean distance based colour image processing	Enhancement	-	-	-	-	-
	Segmentation	Average intensity is 0.9725 in R, G and B domains, Threshold = 0.32			Average intensity is 0.8157, 0.2078 & 0.1922 in R, G & B, Threshold = 0.07	
	Dilation	-	-	-	-	-
	Region filling	-	-	-	-	-
	Erosion	-	-	-	-	-

defect (depth of penetration and tungsten inclusion), the choice (image enhancement and segmentation masks), and shape and size of these factors are different thus making this technique image dependent.

Hotspot extraction from depth of penetration thermographs by region growing, does not involve image enhancement, dilation, region growing and erosion. Hence parameter dependency is less. The only factors involved are selection of seed pixel and threshold. The choice, shape and size of these factors are common to all the three different images depicting depth of penetration. Hence, this technique is also image independent for hotspot extraction. However, this technique involves dilation, region growing and

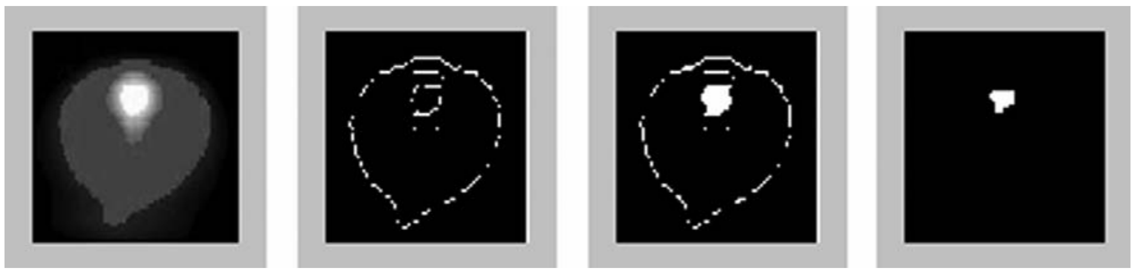

Fig. 6—Gray scale, image, edge detected, region filled and hotspot isolated images for depth of penetration (100 %) thermograph

Fig. 7—Gray scale, image, edge detected, region filled and hotspot isolated images for depth of penetration (80 %) thermograph

Fig. 8—Gray scale, image, edge detected, region filled and hotspot isolated images for depth of penetration (60 %) thermograph

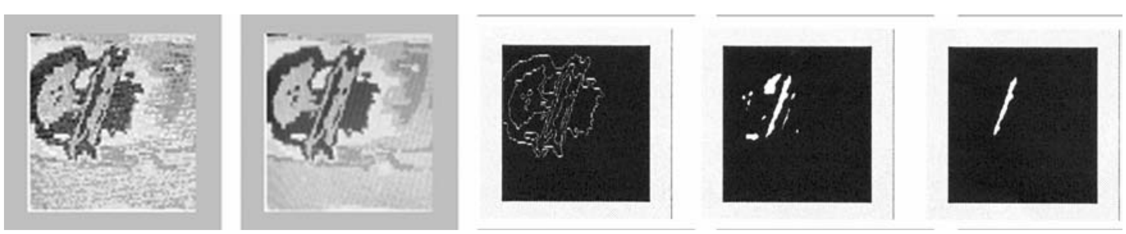

Fig. 9—Gray scale, enhanced image, edge detected, region filled and rod shaped tungsten isolated image

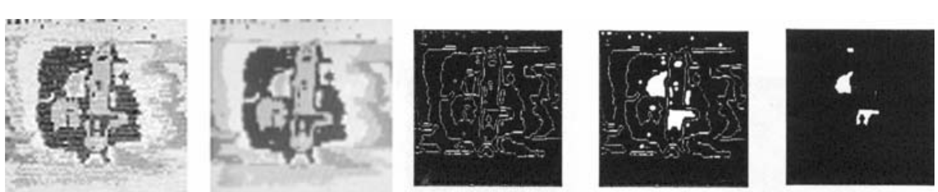

Fig. 10—Gray scale, enhanced Image, edge detected, region filled and gauge shaped tungsten isolated image

erosion for included tungsten extraction thereby making it parameter dependent. Also the size of the structuring elements is different for images depending on the shape of the included tungsten (rows 10-12).

Euclidean distance based colour image segmentation does not involve image enhancement, dilation, region growing and erosion thereby making it parameter independent for both depth of penetration and tungsten inclusion thermographs. Feature extraction is dependent only on average pixel intensities and threshold value. Also these values are same for images of same defect thereby making it image independent.

Discontinuity based technique and region growing involved colour to gray scale conversion which adds quantization error while working on pseudo colour thermographs. On the other hand Euclidean distance based technique works directly on colour images. Hence, Euclidean distance based technique is best suited for pseudo colour thermographs as it does not involve colour to gray scale conversion and is also best suited for automated defect feature extraction as it is image independent and parameter independent.

The output images from discontinuity based detection during extraction of hotspots for 100%, 80% and 60% depths of penetration are shown in Figs 6-8. The output images at different stages of the algorithm for rod shaped tungsten inclusion and gauge shaped tungsten inclusion are as shown in Figs 9 and 10 respectively.

The hotspot extracted output images for different depths of penetration (100%, 80% and 60%) by region growing are shown in Fig. 11. The output images of this technique for rod shaped and Gauge shaped Tungsten Inclusion are shown in Figs 12 and 13.

The output hotspot images for different depths of penetration and included tungsten isolated images by Euclidean distance based colour image segmentation are as shown in Figs 14 and 15 respectively.

The quantitative characterization of the defects is as shown in Table 2.

In discontinuity based detection, hotspots depicting depth of penetration, rod and gauge shaped included tungsten are isolated, extracted and quantified successfully. However, undesirable pixels are also

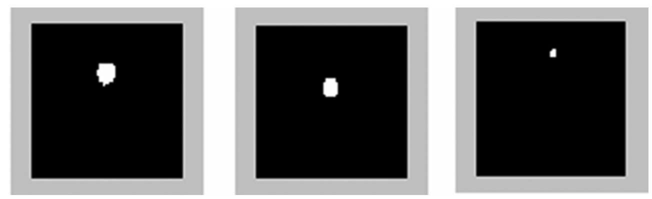

Fig. 11—Hotspot extracted image for 100%, 80% and 60% depth of penetration by region growing

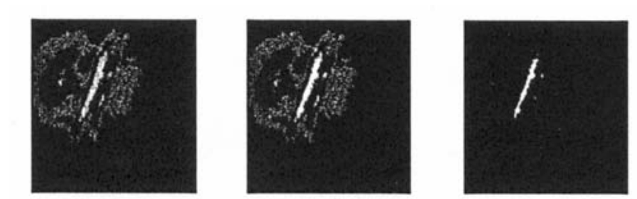

Fig. 12—Appended, region filled and output image for rod shaped tungsten Inclusion detection by region growing

Fig. 13—Appended, region filled and output image for gauge shaped tungsten inclusion detection by region growing

Table 2—Quantitative characterization of defects from feature extraction techniques

Feature extraction techniques	Feature descriptors	Depth of penetration			Tungsten inclusion	
		100%	80%	60%	Rod shaped	Gauge Shaped
Discontinuity based detection	Major axis length	16.2663	9.8274	5.7735	137.0795	44.1997
	Minor axis length	11.5435	9.1034	4.6188	13.1303	25.4830
	Area	138	66	20	1227	699
Region growing	Major axis length	17.9261	13.7970	5.3992	124.5572	51.0308
	Minor axis length	14.3569	13.7470	2.2628	10.6412	27.6422
	Area	198	147	9	771	551
Euclidean Distance based color image segmentation	Major axis length	17.6189	13.9504	4.2307	130.7294	55.1452
	Minor axis length	14.4214	13.6640	3.6870	11.5709	28.0009
	Area	196	148	11	784	526

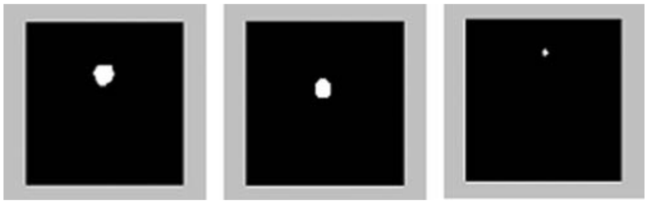

Fig. 14—Hotspot extracted image for 100%, 80% and 60% depth of penetration by Euclidean distance based color image segmentation

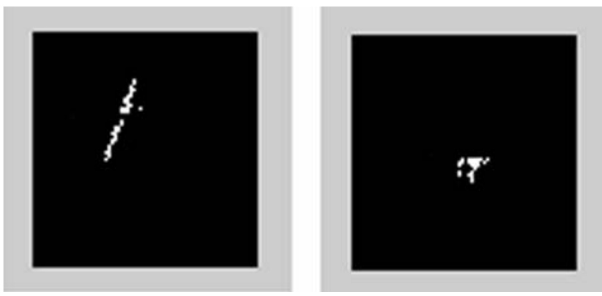

Fig. 15—Rod shaped and gauge shaped tungsten isolated images by Euclidean distance based color image segmentation technique

present. It is because the chosen structuring elements can only best approximate the defect region. Region growing technique worked successfully for hotspot extraction in different depth of penetration thermographs. However, region growing technique as it involved morphological image processing, undesirable regions are present. Euclidean distance based colour image segmentation technique provides better results for both hotspot extraction and tungsten inclusion detection.

Conclusions

Effective feature extraction techniques are developed for defect feature extraction and quantification. Also the suitability of these techniques for automated defect feature analysis is discussed. Discontinuity based technique is parameter independent and image specific and is not suitable for automated analysis. Region growing technique involves a global seed pixel intensity and threshold for all images of different depths of penetration. Hence, this technique is image independent and can be generalized for certain defects (hotspot extraction). However, this technique again involved morphological image processing operators for tungsten inclusion thermographs. Hence became image dependent and cannot be generalized for tungsten inclusion. The above two techniques are best suited for gray scale images. On the other hand if colour thermographs are input images, these techniques involve colour to gray scale conversion which introduced quantization error. Euclidean distance based colour image segmentation algorithms works directly on color images. This technique involves choosing a global threshold value dependent on the nature of the defect. Hence this technique can be generalized and standardized for all colour thermographs of same defect.

References

1 Khan M A, Madsen N H, Goodling G S & Chin B A, *Opt Eng*, 25 (1986) 799-805.

2 Nagarajan S, Chen W H & Chin B A, *Weld J*, 68 (1989) 462s-466s.

3 Groom K N, Nagarajan S & Chin B A, *Weld Res, Suppl Weld J*, (1990) 441s-445s.

4 Chen W & Chin B A, *Weld Res Suppl*, (1990)181s-185s.

5 Nagarajan S, Wikle H C & Chin B A, *J Nuclear Mater*, 191-194 (1992) 1060-1064.

6 Banarjee P, Govardhan S, Wikle H C, Liu J Y, Chin B A, *J Eng Ind*, 117 (1995) 323-330.

7 Ibarra-Castanedo C, Galmiche F, Darabi A, Pilla M, Klein M, Ziadi A, Vallerand S, Pelletier J-F, Maldague X, in *SPIE Proc Thermosense XXV 5073: 450-459*, edited by Orlando, Maldague X, Rozlosnik A, (Florida, USA), 2003.

8 Maldague X, *Mater Evalat*, 6(9) (2002) 1060-1073.

9 Maldague. X, in *Trends in optical nondestructive testing*, edited by Rastogi Pramod, (2000) 591-609.

10 Duncan Camilleri *et al.*, Use of thermography to calibrate fusion welding procedures in virtual fabrication applications, *Inframation-2004 Proc*, ITC 104 A 2004-07-27.

11 Venkataraman B, Baldev Raj & Menaka M, *Mater Evaluat*, (2005) 933-937.

12 Ibarra-Castanedo C *et al.*, Automatic algorithm for quantitative pulsed phase thermography calculations, *Proc 16th WCNDT-World Conf Non-destructive Testing*, Montreal (Quebec), 2004.

13 Shepard S *et al.*, Quantitative characterization of thermo-graphic sequence data, *www.ndt.net/article/wcndt2004*

14 Rafael C Gonzalez & Richard E Woods, *Digital image processing*, (Prentice Hall of India, 2005).